PHYSICAL REVIEW B **82**, 180402(R) (2010)

Spin- and orbital-moment compensation in the zero-moment ferromagnet $Sm_{0.974}Gd_{0.026}Al_2$

S. S. Dhesi,[1,2] G. van der Laan,[1] P. Bencok,[1,2] N. B. Brookes,[2] R. M. Galéra,[3] and P. Ohresser[2,4]
[1]*Diamond Light Source, Chilton, Didcot, Oxfordshire OX11 0DE, United Kingdom*
[2]*European Synchrotron Radiation Facility, BP 220, 38043 Grenoble Cedex, France*
[3]*Institut Néel, Centre National de la Recherche Scientifique, Université Joseph Fourier de Grenoble, BP 166X, 38042 Grenoble Cedex, France*
[4]*Synchrotron SOLEIL, BP 48, 91192 Gif-sur-Yvette, France*

(Received 27 April 2010; revised manuscript received 31 August 2010; published 5 November 2010)

The balance between the orbital and spin magnetic moments of Sm^{3+} in the zero-moment ferromagnet $Sm_{0.974}Gd_{0.026}Al_2$ has been studied using x-ray magnetic circular dichroism (XMCD) at the Sm $M_{4,5}$ edges. The difference in the XMCD multiplet structure below and above the compensation point, T_{comp}, demonstrates that the exchange and crystal-field interactions mix the low-lying $J=7/2$ excited state into the Sm f^5 $^6H_{5/2}$ ground state. Sum-rule analysis of the temperature-dependent XMCD reveals an anomalous change in the Sm^{3+} orbital to spin magnetic-moment ratio as the net magnetization vanishes at T_{comp}. This behavior is ascribed to the role of the conduction electron-spin moment which couples parallel to the Sm spin moment.

DOI: 10.1103/PhysRevB.82.180402 PACS number(s): 75.50.Cc, 78.70.Dm

Spin ordering is often described as ferromagnetic, antiferromagnetic, or ferrimagnetic, where only the ferromagnetic case exhibits a net magnetization without exception. Rare-earth (RE) based intermetallics have been studied for decades[1] but recently it was discovered that Gd-doped $SmAl_2$ can be driven into a state of ferromagnetic spin ordering without exhibiting a net magnetization.[2] $Sm_{1-x}Gd_xAl_2$ relies on the peculiar magnetic properties of the Sm^{3+} ion which possesses oppositely oriented spin ($\mu_S=\langle 2S_z\rangle$) and orbital ($\mu_L=\langle L_z\rangle$) magnetic moments that almost cancel. In addition, second-order Zeeman splitting terms, as described by Van Vleck, affect the magnetic susceptibility since the Sm^{3+} ion has a low-lying $^6H_{7/2}$ excited state. This excited state is able to mix into the $^6H_{5/2}$ ground state so that the temperature dependence of μ_S and μ_L becomes different and the compensation between the two can be enhanced for specific cases. $Sm_{0.974}Gd_{0.026}Al_2$ has a Curie temperature of ~120 K and a compensation temperature, T_{comp}, of ~65 K, at which point the net magnetization vanishes but the ferromagnetic ordering is believed to persist.[3] To date, the exact nature of the mechanism leading to the vanishing magnetization remains unclear with a switching between the Sm^{3+} μ_S and μ_L magnetic moments and a compensation by the spin moments arising from the Gd $4f$ and the delocalized conduction electrons all being considered.[2,4–8]

X-ray magnetic circular dichroism (XMCD) is an ideal probe to study the delicate balance between the Sm^{3+} orbital and spin magnetic moments due to the development of powerful sum rules.[9] XMCD has allowed direct access to impurity magnetism and the magnetocrystalline anisotropy at an unprecedented level.[10] In particular, itinerant $3d$ transition metals have been studied extensively due to the intense $2p$ to $3d$ electric dipole transition, which directly probes the states responsible for magnetism. On the other hand, the highly localized RE $4f$ states have received less attention, even though RE systems were among the first to benefit from polarized x-ray spectroscopy.[11] In part, this may be because sum-rule analysis for REs requires further refinement due to intensity transfer between spin-orbit split edges. However, XMCD has been applied to Gd-doped $SmAl_2$ and confirmed the persistence of long-range order for both μ_L and μ_S. On the other hand, sum-rule analysis showed almost no change in the ratio of μ_L to μ_S at T_{comp} which is surprising and could be ascribed to a magnetically unsaturated sample.[5,6]

Here, we use XMCD to investigate the temperature dependence of both the J mixing and the orbital and spin magnetic-moment balance of the Sm^{3+} ions in $Sm_{0.974}Gd_{0.026}Al_2$. High-resolution XMCD spectra measured at low and high temperature in a field of 7 T are compared with atomic multiplet calculations and evidence the presence of the J mixing in the Sm^{3+} ground state. Furthermore, XMCD sum-rule analysis reveals that the Sm^{3+} orbital to spin magnetic-moment ratio exhibits large changes near the compensation point. This suggests that the conduction electrons provide the principle driving mechanism behind the observed zero-moment magnetization.

The $Sm_{0.974}Gd_{0.026}Al_2$ was prepared by induction melting. X-ray diffraction showed that a single-phase sample was produced. Superconducting quantum interference device magnetometry showed that the magnetic behavior of the $Sm_{0.974}Gd_{0.026}Al_2$ was identical to that of previous studies.[2] Clean surfaces were prepared *in situ* by filing of polycrystalline samples with a diamond file. The samples were inserted into a 7 T superconducting magnet operating in a UHV environment. X-ray absorption (XA) spectroscopy and XMCD measurements were performed using circularly polarized light at beamlines ID12B and ID08 of the European Synchrotron Radiation Facility (ESRF) in Grenoble. The XMCD was obtained, using total electron yield, by switching either the sample magnetization, **M**, or the helicy vector of the incident radiation, **P**, in order to remove any small systematic errors. The XA spectra were normalized to a constant edge jump in order to yield information on a per atom basis. Saturation effects in XA are known to be significant for RE metals over the soft x-ray energy range[12] so that angle-dependent measurements above the Curie point were used to eliminate the influence of these effects.

Figure 1(a) shows the Sm $M_{4,5}$ XA spectrum for $Sm_{0.974}Gd_{0.026}Al_2$ recorded at $T=10$ K. The detailed line

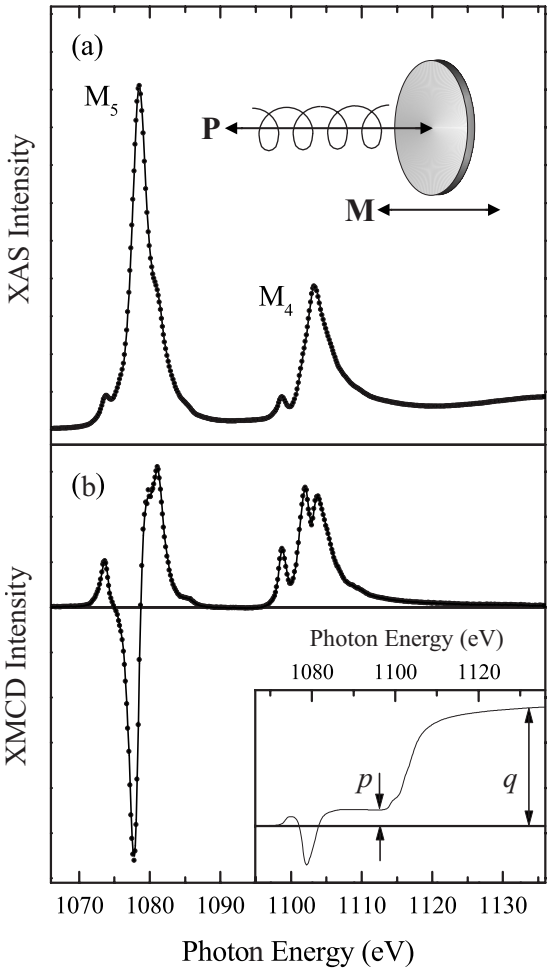

FIG. 1. Sm $M_{4,5}$ spectra of $Sm_{0.974}Gd_{0.026}Al_2$ recorded at $T=10$ K. (a) XA spectrum. Also the experimental geometry is shown, where the double-headed arrows indicate that either the helicity vector, **P**, or the magnetization, **M**, can be reversed. (b) The difference between two XA spectra recorded with **M** parallel and antiparallel to **P**, i.e., the XMCD. The inset shows the integral of the XMCD spectrum, where p is the integral over the M_5 edge and q is the integral over both the M_4 and M_5 edges.

shape of the XA spectrum confirms the trivalent nature of the Sm.[12] The spectrum reveals a multiplet structure that is characteristic for the electric-dipole transition $4f^5 \rightarrow 3d^9 4f^6$.[13] Figure 1(b) shows the difference, i.e., the XMCD, between the XA spectra recorded with **M** applied parallel and antiparallel to **P**. The same spectrum is obtained regardless of whether **M** or **P** is reversed during the measurement. The XMCD exhibits an intense negative feature at the M_5 edge with more structured positive features at the M_4 edge.

We will first discuss the effect of J mixing. The Sm $4f^5$ ground state $^6H_{5/2}$ is split by the crystal-field interaction.[14] In the absence of any J mixing, the μ_L/μ_S ratio will be temperature independent and equal to the atomic ratio.[15] However, the first-excited state $J=7/2$ is at ~ 1000 cm^{-1} (~ 1400 K), which mixes into the ground state by exchange and crystal-field interactions. Off-diagonal matrix elements will already cause a substantial contribution at moderate temperature (atomic matrix elements are given in Table I).

TABLE I. Calculated diagonal and off-diagonal matrix elements $\langle JM|\mathcal{H}|J'M\rangle$ for the orbital and spin magnetic moments and magnetic dipole term, T_z (in μ_B) of the Sm f^5 ground state with $J=5/2$ and $7/2$ for $M=-5/2$.

	$\langle L_z\rangle$	$\langle 2S_z\rangle$	$\langle T_z\rangle$
$\langle \frac{5}{2},-\frac{5}{2}\|\mathcal{H}\|\frac{5}{2},-\frac{5}{2}\rangle$	−4.25	3.50	−0.39
$\langle \frac{5}{2},-\frac{5}{2}\|\mathcal{H}\|\frac{7}{2},-\frac{5}{2}\rangle$	0.95	−1.90	0.03
$\langle \frac{7}{2},-\frac{5}{2}\|\mathcal{H}\|\frac{7}{2},-\frac{5}{2}\rangle$	−2.92	0.84	−0.23

Due to the J mixing, the orbital and spin magnetic moment will both reduce gradually with increasing temperature and also the μ_L/μ_S ratio is expected to decrease.

Experimental evidence for the J mixing is provided by the change in multiplet structure of the XMCD. Figure 2(a) shows the XMCD spectra recorded above and below T_{comp}. The most pronounced difference in the M_5 and M_4 edge is observed at ~ 1079 eV and ~ 1104 eV, respectively. The difference of the two XMCD spectra is shown in Fig. 2(b). This is compared with the calculated difference between high- and low-temperature XMCD spectra, showing an excellent agreement. For the multiplet structure, calculated in intermediate coupling, the parameters were taken as in Ref. 12, with the Slater integrals reduced to 80% and the $3d$ spin-orbit interaction reduced to 95% of the Hartree-Fock values.[13] Thus, the temperature-dependent change in the XMCD is clear proof for the J mixing. Although the J mixing is facilitated by the crystal-field interaction, the multiplet structure is insensitive to the details of the crystal field, because this interaction is small compared to the spin-orbit and electrostatic interactions. The crystal field also changes the spin and orbital moments,[14] which via the sum rules[9] can be determined from the integrated intensities of the M_4- and M_5-edge XMCD.

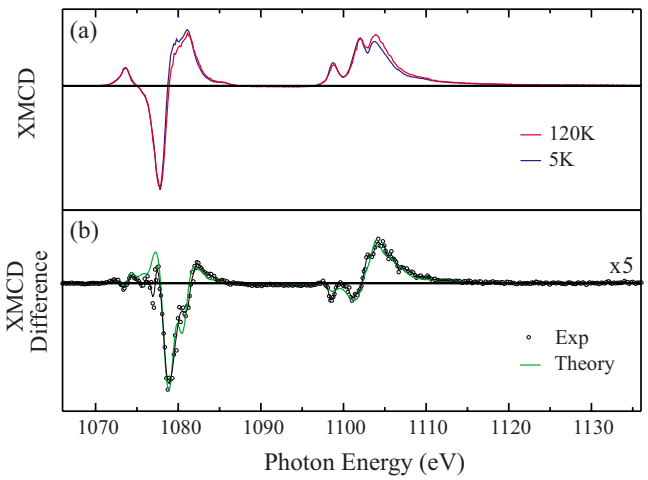

FIG. 2. (Color online) (a) Sm $M_{4,5}$ XMCD spectra recorded at 120 K and 5 K in a 5 T field. The spectrum recorded at 120 K has been inverted to allow comparison and both spectra have been normalized to the minimum XMCD at the M_5 edge. (b) Difference between the XMCD spectra shown in (a) (open circles with solid black line) together with the calculated difference spectrum [green (gray) line] for high and low temperature using an atomic multiplet calculation.

Although, the sum rules can yield the separate values of μ_S and μ_L, here we determine their relative values as we are mainly interested in the balance between these moments. This is also a more straightforward procedure since it does not require the integrated intensity of the isotropic spectrum. The inset of Fig. 1(b) shows the integral of the XMCD spectra, where p represents the integral over the M_5 edge and q the integral over both edges. q is directly proportional to μ_L, whereas the branching ratio p/q can be used to determine μ_L/μ_S.[9] However, the $3d$-$4f$ Coulomb interaction in the RE is relatively large compared to the $3d$ core-level spin-orbit interaction. This leads to the so-called jj mixing, i.e., a mixing of the $j=5/2$ and $j=3/2$ core-level manifolds.[13] The corrected sum rules for the rare earths $M_{4,5}$ edges can be written as,[15]

$$\frac{\mu_L}{\mu_S} = \frac{2C}{5\frac{p}{q} - 3}\left(1 + \frac{6\langle T_z\rangle}{\mu_S}\right), \tag{1}$$

where C is the correction factor due to jj mixing. In rare earths the contribution of the magnetic dipole term, T_z, to the sum rule can be substantial. Atomic multiplet calculations for Sm^{3+} give $\langle T_z\rangle/\mu_S = -0.11$, in good agreement with the experimental result of −0.09 obtained for $SmAl_2$.[16] The spin-orbit interaction couples T_z antiparallel to S_z and at the compensation point both $\langle S_z\rangle$ and $\langle T_z\rangle$ will reverse in sign. The values of μ_S, μ_L, $\langle T_z\rangle$, and to a lesser degree C are temperature dependent. Assuming that the temperature dependence of the ratio μ_L/μ_S is much stronger than that of C and $\langle T_z\rangle/\mu_S$ (cf., Table I), as is confirmed by theoretical calculations,[5] Eq. (1) can be written approximately as

$$\frac{\mu_L}{\mu_S} \approx \frac{2C'}{5\frac{p}{q} - 3}. \tag{2}$$

By comparing calculated XMCD spectra with their corresponding calculated ground-state magnetic moments using the Cowan's code,[17] we derive a correction factor of $C' \approx 1.14$ for the $M_{4,5}$ edges of the Sm f^5 configuration.

Figure 3 shows the temperature dependence of the integral q ($\propto \mu_L$) determined by cooling the sample to 10 K in a 5 T field followed by measuring the XMCD, with increasing temperature, by switching both **P** and **M** at each temperature. There is a clear change in the sign of μ_L between 65 and 70 K, implying that the net magnetization of the Sm^{3+} ion has changed direction at $T_{comp} \approx 67$ K. The net sample magnetization is proportional to $\mu_S + \mu_L + \mu_{ce} + \mu_{Gd}$, where μ_S and μ_L are the local spin and orbital moments specific to the Sm atom (and measured by XMCD) while μ_{ce} is the spin moment of the conduction electrons and μ_{Gd} is the spin moment due to the Gd. The moments of μ_{ce} (~0.24 μ_B) and μ_{Gd} (~7.6 $\mu_B \times 0.026$) are parallel to μ_S, which is antiparallel to μ_L.[18] Previous studies have implied that the zero-moment magnetization is due to a delicate balance between μ_S, μ_L, μ_{ce}, and μ_{Gd}. Figure 3 shows that μ_L changes at $T \approx 67$ K from parallel to antiparallel alignment to the net magnetization, therefore $-\mu_L > \mu_S + \mu_{ce} + \mu_{Gd}$ below T_{comp} and $-\mu_L < \mu_S + \mu_{ce} + \mu_{Gd}$ above T_{comp}. The low- and high-

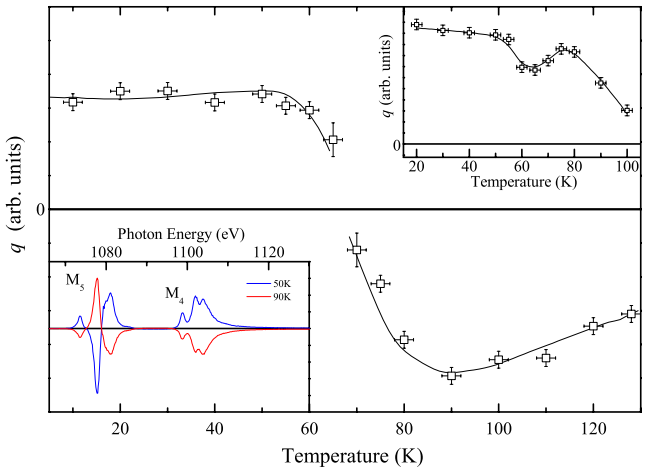

FIG. 3. (Color online) Temperature dependence of the integral q ($\propto \mu_L$) of the Sm $M_{4,5}$ XMCD spectra. The lines are guide to the eyes. The lower inset shows the change in sign of the XMCD spectra as the sample is warmed through T_{comp} in a 5 T field. The upper inset shows q as the sample is warmed up in zero field.

temperature XMCD spectra (lower inset of Fig. 3) show the reversal of the XMCD spectra as the sample is warmed up in a magnetic field. On the other hand, the upper inset of Fig. 3 shows μ_L as the sample is warmed up in zero field after applying a field of 5 T at 10 K. The Sm orbital moment therefore persists at T_{comp} but does not change sign since the reversal of the magnetization at T_{comp} cannot overcome the magnetic anisotropy in the absence of a field.

Figure 4 shows the temperature dependence of μ_L/μ_S obtained from the Sm $M_{4,5}$ XMCD using Eq. (2). For comparison, also shown is the temperature dependence for $SmAl_2$ and $Sm_{0.939}Nd_{0.061}Al_2$, determined using XMCD, demonstrating that there is no change in μ_L/μ_S for these materials. For $SmAl_2$, μ_L/μ_S is found to be 1.14 ± 0.01, in good agreement with previous studies[18,19] and close to the calculated

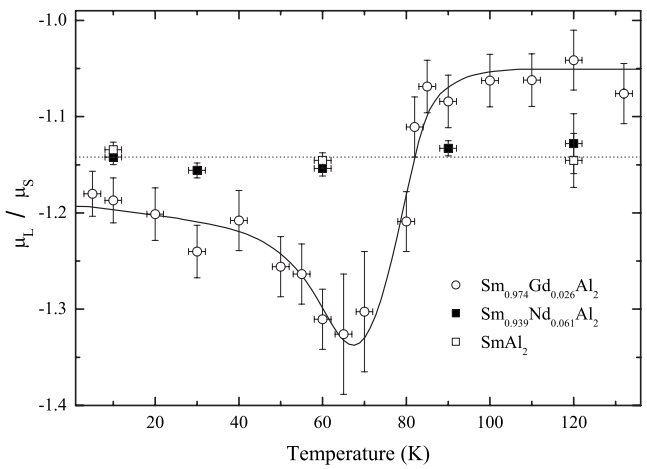

FIG. 4. Ratio of the orbital to spin magnetic moments, μ_L/μ_S, as a function of temperature for $Sm_{0.974}Gd_{0.026}Al_2$ (open circles), $SmAl_2$ (open squares), and $Sm_{0.939}Nd_{0.061}Al_2$ (closed squares) measured in 5 T field. The solid line is a guide to the eyes, whereas the broken line is the average value found for $SmAl_2$. The μ_L/μ_S value has been obtained using Eq. (2) in all cases.

atomic ratio of 1.2 (cf., Table I). Since $|\mu_L/\mu_S|>1$, the orbital moment always exceeds the spin moment, so that the μ_{ce} and μ_{Gd} contributions to the total spin moment are essential to compensate the Sm orbital moment. Since μ_{Gd} is aligned parallel to μ_S, it acts to effectively increase μ_S at all temperatures as demonstrated using XMCD.[5,6,20] On the other hand, while it has previously been assumed that μ_L/μ_S for Gd-doped $SmAl_2$ gradually decreases with increasing temperature, Fig. 4 shows a more complicated behavior at and above T_{comp}.

Compared to $T=10$ K, there is a $\sim 10\%$ increase in μ_L/μ_S at T_{comp}. The origin of this enhancement is expected to be related to the vanishing net magnetization at T_{comp}. This can result in either a reduced local Sm spin moment or an enhanced Sm orbital moment caused by the increased level degeneracy. The coercivity has been shown to increase as the temperature approaches T_{comp} implying a decrease in the spin moment[3] around T_{comp}. In addition, the inset of Fig. 3(a) XMCD confirms that μ_L also changes around T_{comp}. Since the $4f$ spin-orbit interaction imposes antiparallel spin and orbital moments, canting of the spin moment can be excluded. Above T_{comp}, μ_L/μ_S rapidly increases to a steady value at ~ 85 K. Above this temperature the orbital moment will be outweighed by the net spin moment. Using values of μ_{ce} from Adachi *et al.*[18] the compensation is expected at $\mu_L/\mu_S \approx -1.12$. This implies that for the region $67<T<80$ K, where the net Sm spin moment is not sufficient to compensate the orbital moment, the interaction with the conduction electrons is important. Since the atomic Sm f^5 configuration can only give a monotonic decrease in μ_L/μ_S as a function of temperature, long-range ordering of the spin moments must play an important role. In particular, the temperature-dependent conduction electron contribution must compensate the increase in μ_L/μ_S at T_{comp} indicating a more complex coupling between μ_{ce}, μ_L, and μ_S over an extended temperature range close to T_{comp} than previously proposed.[20] The detailed XMCD over the Sm $M_{4,5}$ edges in this work, therefore, suggests a small modulation ($<0.05\mu_B$) of the conduction-band magnetic moment around T_{comp}. Such a modulation implies a change in the electronic structure around T_{comp} resulting in a specific-heat anomaly which has recently been observed.[7]

Summarizing, we employed XMCD to study the orbital and spin magnetic moments of Sm^{3+} in the zero-moment ferromagnet $Sm_{0.974}Gd_{0.026}Al_2$. The differences in the XMCD multiplet structure for low and high temperature can be ascribed to J mixing by comparing the spectra to atomic calculations. Sum-rule analysis of the XMCD reveals an anomalous temperature dependence of the orbital to spin magnetic-moment ratio. The magnitude of the orbital moment is enhanced compared to the spin moment at T_{comp} and in a finite range above T_{comp}. In order to completely compensate the total magnetization at T_{comp} a small modulation of the conduction electron magnetic moment is required.

We thank staff at the European Synchrotron Radiation Facility (ESRF) in Grenoble, particularly K. Larsson, for help and technical assistance.

[1] A. K. Grover *et al.*, J. Appl. Phys. **50**, 7501 (1979).
[2] H. Adachi and H. Ino, Nature (London) **401**, 148 (1999).
[3] H. Adachi, H. Kawata, H. Hashimoto, Y. Sato, I. Matsumoto, and Y. Tanaka, Phys. Rev. Lett. **87**, 127202 (2001).
[4] J. W. Taylor, J. A. Duffy, A. M. Bebb, M. R. Lees, L. Bouchenoire, S. D. Brown, and M. J. Cooper, Phys. Rev. B **66**, 161319 (2002).
[5] S. Qiao *et al.*, Phys. Rev. B **70**, 134418 (2004).
[6] S. Qiao *et al.*, Physica B **351**, 333 (2004).
[7] X. H. Chen, K. Q. Wang, P. H. Hor, Y. Y. Xue, and C. W. Chu, Phys. Rev. B **72**, 054436 (2005).
[8] A. Avisou *et al.*, J. Phys.: Condens. Matter **20**, 265001 (2008).
[9] B. T. Thole, P. Carra, F. Sette, and G. van der Laan, Phys. Rev. Lett. **68**, 1943 (1992); P. Carra, B. T. Thole, M. Altarelli, and X. Wang, *ibid.* **70**, 694 (1993); G. van der Laan, Phys. Rev. B **57**, 112 (1998).
[10] P. Gambardella *et al.*, Science **300**, 1130 (2003).
[11] G. van der Laan, B. T. Thole, G. A. Sawatzky, J. B. Goedkoop, J. C. Fuggle, J. M. Esteva, R. Karnatak, J. P. Remeika, and H. A. Dabkowska, Phys. Rev. B **34**, 6529 (1986).
[12] B. T. Thole, G. van der Laan, J. C. Fuggle, G. A. Sawatzky, R. C. Karnatak, and J. M. Esteva, Phys. Rev. B **32**, 5107 (1985).
[13] G. van der Laan and B. T. Thole, Phys. Rev. Lett. **60**, 1977 (1988); B. T. Thole and G. van der Laan, Phys. Rev. B **38**, 3158 (1988).
[14] K. H. Buschow *et al.*, Phys. Rev. B **8**, 5134 (1973).
[15] G. van der Laan and B. T. Thole, Phys. Rev. B **53**, 14458 (1996).
[16] S. S. Dhesi *et al.*, J. Appl. Phys. **93**, 8337 (2003).
[17] R. D. Cowan, *Theory of Atomic Structure and Spectra* (University of California Press, Berkeley, 1981).
[18] H. Adachi, H. Ino, and H. Miwa, Phys. Rev. B **59**, 11445 (1999).
[19] A. Barla, J. P. Sanchez, F. Givord, J. X. Boucherle, B. P. Doyle, and R. Rüffer, Phys. Rev. B **71**, 012407 (2005).
[20] The expected temperature dependence of the Gd f^7 spin moment was found using XMCD over the Gd $M_{4,5}$ edges.